
**Journal of Macromolecular Science, Part A**
Publication details, including instructions for authors and subscription information:
http://www.informaworld.com/smpp/title~content=t713597274

# Optical and Electronic Properties of Organic Photovoltaic Wires and Fabrics

Michael R. Lee[a]; Robert D. Eckert[a]; Karen Forberich[a]; Gilles Dennler[a]; Christoph Brabec[a]; Russell A. Gaudiana[a]; Paul Calvert[b]; Anshul Agrawal[b]
[a] Konarka Technologies, Inc, Lowell, Massachusetts [b] The University of Massachusetts, North Dartmouth, MA

**To cite this Article** Lee, Michael R. , Eckert, Robert D. , Forberich, Karen , Dennler, Gilles , Brabec, Christoph , Gaudiana, Russell A. , Calvert, Paul and Agrawal, Anshul(2009) 'Optical and Electronic Properties of Organic Photovoltaic Wires and Fabrics', Journal of Macromolecular Science, Part A, 46: 12, 1238 — 1246
**To link to this Article: DOI:** 10.1080/10601320903340465
**URL:** http://dx.doi.org/10.1080/10601320903340465

*Journal of Macromolecular Science®, Part A: Pure and Applied Chemistry* (2009) **46**, 1238–1246

ISSN: 1060-1325 print / 1520-5738 online
DOI: 10.1080/10601320903340465

Taylor & Francis
Taylor & Francis Group

# Optical and Electronic Properties of Organic Photovoltaic Wires and Fabrics

MICHAEL R. LEE[1], ROBERT D. ECKERT[1], KAREN FORBERICH[1], GILLES DENNLER[1], CHRISTOPH BRABEC[1], RUSSELL A. GAUDIANA[1,*], PAUL CALVERT[2] and ANSHUL AGRAWAL[2]

[1]*Konarka Technologies, Inc, 116 John Street, Suite 12, 3rd Floor, Lowell, Massachusetts 01852*
[2]*The University of Massachusetts, Dartmouth, Old Westport Road, North Dartmouth, MA 02747-2300*

The characteristics of a power producing flexible wire based on organic photovoltaics (OPV) and the processes by which they are produced are described in this paper. A set of materials and coating formulations used on the electrode wires are very similar to those used in the development of two dimensional photovoltaic cells and modules. The active layer of the primary electrode wire comprises the bulk heterojunction-forming P3HT/PCBM (1:1 weight ratio) that has been extensively studied in planar cells. A second wire, which is wrapped around the coated, primary electrode wire, serves as the counter electrode. Ray tracing analysis indicates that light incident on the wires is focused by the cladding onto to the active layer, coated, primary electrode wire even when it is completely shadowed by the counter electrode. Furthermore, when the counter electrode is in a position that partially shadows the primary wire, a significant percentage of the light is reflected by the counter electrode onto the primary electrode.

Many hundreds of feet of OPV wire have been produced continuously for experimental purposes, and the process is capable of producing any length of PV wire desired. Efficiency values of a 200 foot spool of PV wire ranges from 2.79% to 3.27%.

**Keywords:** Solar energy, organic photovoltaics, polymer bulk-heterojunction, photovoltaic wires



## 1 Introduction

Since its founding in 2001, Konarka Technologies has been developing thin film, solar modules based on dye sensitized titania and organic photovoltaics. The driving force behind this concentrated activity is the widely held opinion that solar energy represents one of the cleanest sources of renewable power, and it has the potential and the expectation to contribute significantly to the world's energy supply within the next 25–50 years (1, 2). There is currently an intense worldwide effort to develop and produce solar modules and to integrate solar power into all facets of energy production and use. These applications include large area photovoltaic power plants to power supplies for indoor sensors to portable battery chargers. Such a large number of electronic applications requires a truly versatile product from the standpoint of form factor and functionality. The use of organic and hybrid solar cells, based on nanostructured, bulk-heterojunction composites, represents a general approach towards flexible solar cells with reduced costs and size (3–9).

Since the first reports in the early 1990s (3, 10), thin film solar modules based on organic photovoltaic composites have been the focus of many academic and industrial laboratories. The basic concept is to manufacture modules on thin, flexible substrates at high speed using a combination of printing, coating and laminating processes similar to those that have been used in the photographic industry and a wide variety of other coating and printing industries for many decades. The low capital costs and high production rates of these well known processes have the potential to generate megawatts of solar power at unprecedented low cost. Although there are many thin film technologies being developed today, e.g., copper-indium-gallium-selenide (CIGS), amorphous silicon (a-Si), dye-sensitized titania (DSSC), the technology known as Organic Photovoltaics (OPV) represents the greatest potential for achieving the combination of light weight, flexibility, high performance and low cost solar panels that is important to many applications. The key feature of this technology is the unique morphology of the photoactive layer, known as a bulk-heterojunction that was first reported by Sarifciftci, Heeger, et al. (10). This morphology comprises two materials; one is a polymer and the other a solubilized fullerene derivative known in the literature as PCBM ([6,6]-phenyl-$C_{61}$ butyric acid methyl ester). These components, which are for the most part mutually insoluble

*Address correspondence to: Russell A. Gaudiana, Konarka Technologies, Inc., 116 John Street, Suite 12, 3rd Floor, Lowell, Massachusetts 01852. E-mail: rgaudiana@konarka.com

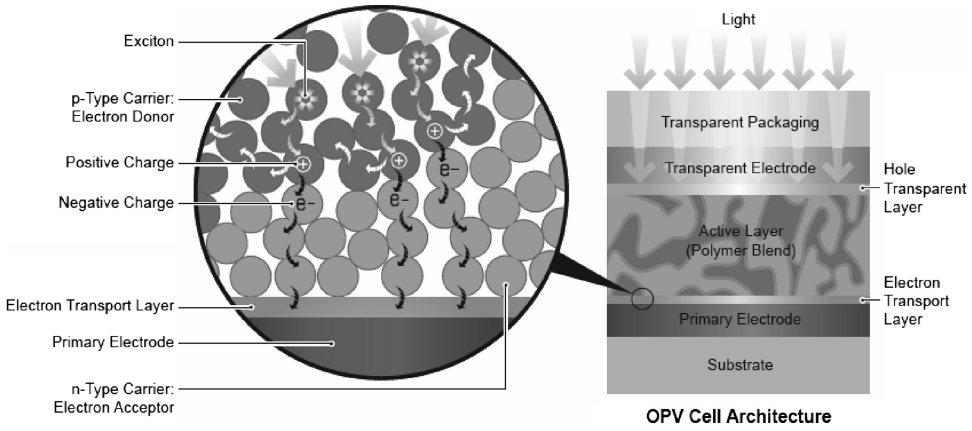


**Fig. 1.** A schematic of a cross-section of an OPV cell and its operating mechanism.

in one another, can be dissolved in a solvent, and when the resulting homogenous solution is coated as a thin layer on a substrate, the polymer and fullerene partially phase separate into intertwined wormlike or channel-like domains (shown schematically in Figure 1). This morphology creates an extremely high surface area between the polymer phase (the electron donor) and the fullerene phase (the electron acceptor) that enhances electron injection.

If the cross-sectional dimension of the channels is in the 20–50 nm range, excitons produced in the polymer phase upon absorption of incident radiation diffuse to the interface with the fullerene phase. At this interface, an electron from the excited state of the polymer is transferred to the fullerene phase. The hole, or cation, on the polymer chain from which the electron was ejected migrates to the transparent electrode by an electron/hole exchange mechanism between neighboring polymer chains. The electron in the fullerene phase hops from one fullerene molecule to another as it moves to the primary electrode. The electrons flow from the primary electrode to an external load, such as a light bulb or a motor, and re-enter the cell via the transparent electrode. At the interface with the transparent electrode, each hole residing on the polymer chain picks-up an electron which converts it back to its ground state thus completing the electrical circuit.

Theoretical studies have shown that the most recent generation of bulk heterojunction composites has an efficiency potential >10% for single junction devices (11) and 15% for dual junction (tandem) devices (12). Moreover, recent theoretical studies have indicated that photovoltaic nanowire structures where the active layer is coaxially embedded between the electrode layers in a p-i-n configuration could improve carrier collection and overall efficiency with respect to planar cell geometry of the same materials (13, 14). However, solar cells on nanowires or nano fibers reported so far suffer from relatively low efficiencies compared to their flat junction references (15).

Since 2002, we have been researching the materials and processes required for making fibers or wires that are capable of producing power from solar and indoor radiation. Our ultimate interest in this application is to produce fabric that can be made into garments, awnings, tarps, sails, draperies, etc. For the first several years of this work, we concentrated on the utilization of dye sensitized titania technology. Although making wires using this technology was very difficult, primarily due to the necessity of encapsulating a liquid electrolyte with a polymeric cladding, we had good success in that we were able to make PV wires that produced power, when irradiated in full sun; this will be the subject of a later publication.

In spite of our success, there are two major problems with DSSC-based wires which are directly related to the nature of the primary components of the cell and which cannot be easily overcome:

1. The sintered titania layer is brittle enough so that when it is bent around a small radius or elongated in excess of 1%, it cracks and flakes off the wire upon which it is coated (16, 17).
2. The liquid electrolyte is sensitive to water ingress, which cannot be prevented by the fairly thin protective outer cladding, and it leaks from the cell through the thin cladding.

In OPV technology, the individual layers are coated from solution and dried thereby making the finished wire completely solid state (18). This feature not only makes the wires much easier to produce, but its applications are much more practical and more diverse than wires comprising dye sensitized titania/liquid electrolyte. One of the major difficulties with OPV wire technology is the thinness of the photoactive coatings which can lead to shunting between the electrodes thus necessitating the use of very a smooth wire core. In addition, a counter electrode comprising an n-type carrier that is both highly conductive, making it capable of carrying current over long distances, and optically transparent, does not exist. As a result, a second wire must be used as the counter electrode in analogy to our DSSC PV wire. In the latter, the problem of making electrical contact

between the wires is alleviated by the highly conductive electrolyte in which the wires are embedded. In OPV, in order to electrically contact the co-axial primary and secondary wires, they must make permanent physical contact. This is accomplished by wrapping the counter electrode around primary electrode under tension while applying and polymerizing the cladding. Having overcome these problems, 300–400 foot spools of OPV-based wires have been made continuously, and they have been woven into fabrics.

### 1.1 Coating Processes and Wire Architecture

In the following sections, we describe the processes, structure, characteristics and performance of a new form and use for organic photovoltaics, namely, co-axial OPV wires. The basic idea is to use one wire as the primary electrode and successively coat all three of the photocell layers, e.g., the electron transport layer, the photo-active layer and the hole transport layer, in sequence on top of one another placing layer upon layer around the core wire. Each of the coatings is deposited by drawing the core wire through a series of coating cups and drying ovens. The counter electrode wire is wrapped around the coated core wire. The outer-most layer is a transparent, protective polymer cladding (19).

One of the biggest problems for photovoltaic fibers, which necessitates the use of a counter electrode wire, is the collection of carriers and the transport of current by a transparent, conductive coating over distances in the range of at least 10–20 cm which is the minimum length required for the first applications. Even ITO coatings with a surface resistivity as low as 10 ohms/cm$^2$ cannot transport the photocurrent generated with 1 sun irradiance over more than 10–15 mm without incurring electrical losses. We therefore decided to split the transport problem into two parts. The first part requires the transport and collection of hole carriers around the primary wire, while the second part requires the transport of electrons along the wire. Hole carriers in the very thin PV layers of the wire (circumference = 314 $\mu$m — the diameter of the primary electrode wire is 100 $\mu$m (Fig. 2) must travel no more than 157 $\mu$m to reach any point on the outer circumference. Hence, a coating with a surface resistivity of 1 kohm/cm$^2$ is sufficient for efficient collection. The highly conductive hole transport layer, e.g., PEDOT (conductivity $\sim$10 S/cm), can easily fulfill this requirement, and its transmission is $>$85% in the visible region of the spectrum. The second transport problem requires the conduction of electrons over long distances. The metal primary electrode wire provides this level of conductivity. The idea that a second wire can be used to conduct electrons, provided that it contacts the surface of the primary wire along both of their lengths, was perhaps the key concept for making practical PV wires.

To begin the process of building an OPV wire, a stainless steel wire, which serves as the primary electrode, is coated



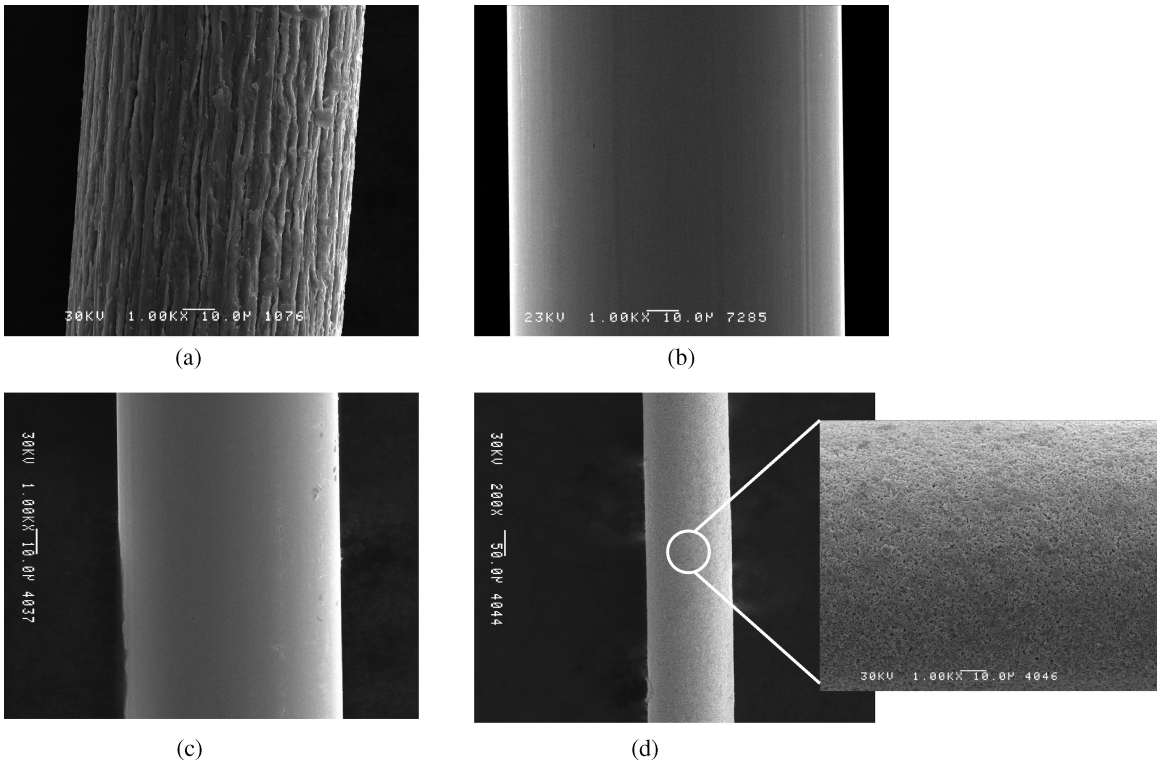


**Fig. 2.** Scanning Electron Micrographs of: (a) the surface of 4 mil titanium wire; (b) 4 mil 316 stainless steel wire extruded through a diamond orifice; (c) ordinary 2 mil 316 stainless steel wire; (d) silver-clad 2 mil wire (blow-up of silver surface).

with the photoactive layers. Stainless steel (ultra-smooth, 316 grade) was chosen over other metals because it exhibits a very useful combination of properties. It has high break strength, e.g., 470 g, at small diameters (100 $\mu$m, 0.004") and good conductivity (resistance = 94 ohms/meter).

Another factor that led us to choose stainless steel wire is its surface roughness. Because the sum of the thicknesses of the PV coatings on the core wire is <250 nm, the surface features of the wire upon which these layers are placed must be in this range. Figure 2 shows scanning electron microscope pictures of the surfaces of two wires before coating. The image on the left shows the surface of a 4 mil titanium wire (Fig. 2a) (Perryman, Houston, PA); clearly the surface is extremely rough with surface features that are much greater than the submicron coatings of the OPV layers. Due to the hardness of this metal, the wire cannot be made any smoother according to the manufacturers. The wire on the right (Fig. 2b) is 4 mil, 316 stainless steel that was extruded through a diamond orifice (Fort Wayne Metals, Fort Wayne, IN). The surface is significantly smoother, and this is the wire that is now used as the primary electrode. Figure 2(c) is an SEM of 2 mil stainless wire that is now used for the secondary electrode. The surface roughness is very good, but does contain bumps and rough areas that precludes its use as the primary electrode. In addition, it has much poorer conductivity and low break strength (resistance = 374 ohms, 118 g). In order to use this wire as the secondary electrode, its conductivity had to be increased, and for this reason we coated it with a thin layer of silver paste comprising both plate-like and irregularly shaped silver particles by drawing it through a coating cup. Upon drying at 120°C, the silver particles contact one another so as to produce a smooth, uniform, 1 mil thick conductive sheath of silver around the wire (Fig. 2d). The resistance of a 1 meter long wire is 115 ohms which makes it nearly as good as 4mil stainless wire. The wire is taken up on a spool before joining it to the primary wire.

As previously mentioned, the PV layers are coated successively on one another by means of a series of vertically aligned coating cups containing the coating solutions of each successive layer. The coating speeds range from 10 feet/minute to as high as 50 feet/minute. Each coating cup has a hole in the bottom; the diameter of the hole is slightly larger than the diameter of the wire which allows the wire to pass through without touching the walls of the orifice. In this process, the primary wire is drawn through a cup containing an isopropanol solution of tetra(n-butyl)titanate, after which, it immediately enters an oven (90–100°C) which drives off the solvent. This process forms a smooth, thin, robust layer of TiOx which serves as the electron transport layer. Next, the coated wire is drawn through a second coating cup containing a solution of the active layer, which in these examples is a 1:0.8 (wt/wt) mixture of poly(3-hexyl-2,5-thiophene) (P3HT, Merck KGaA, Darmstadt, Germany) and ([6,6]-phenyl-$C_{61}$ butyric acid methyl ester) ($PC_{61}BM$, Solenne BV, Groningen, Netherlands). This coating is then dried in a second oven set at 120°C. The procedure is repeated for the hole transport layer, i.e., electron blocking layer, which is typically poly(3,4-ethylenedioxylenethiophene-polystyrne sulfonate (PEDOT·PSS, Baytron P HC V4, H. C. Stark, Newton, MA) or one of its analogues. The completed wire is shown schematically in Figure 3.

The preparation of the secondary wire is described above. The idea that a second wire could be used as the secondary electrode, provided that it would contact the surface of the primary wire along both of their lengths, was perhaps the key concept for making practical PV wires. The idea was first demonstrated with the DSSC-based PV wire. In this case, the highly conductive liquid electrolyte helped to

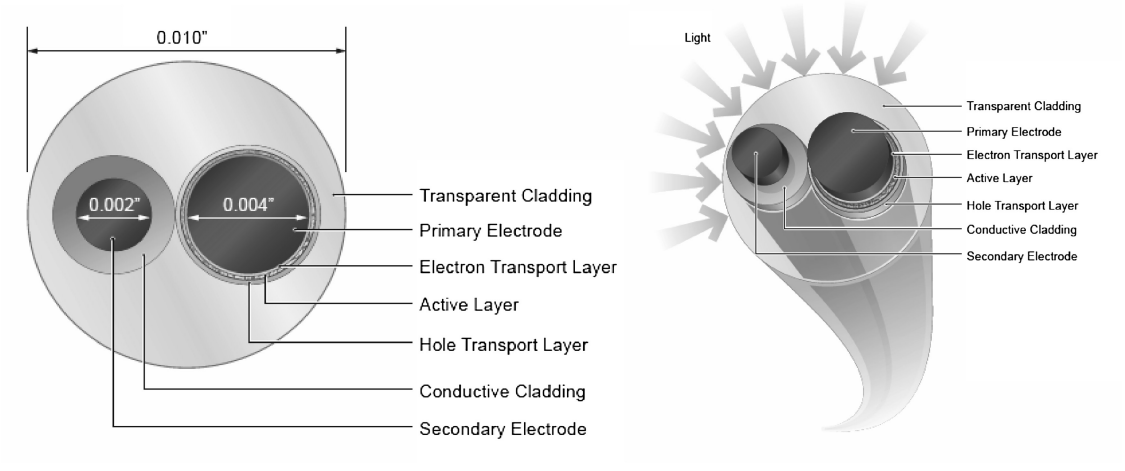


(a) (b)

**Fig. 3.** (a) End-on schematic view of an OPV wire with the dimensions of the electrode wires and the coated layers; the photoactive layers on the primary electrode are not drawn to scale; (b) complete fiber showing the potential for shadowing by the secondary electrode.

ensure that the parallel-aligned electrode wires contacted each other, and in places where they did not make contact directly, the electrolyte provided a shuttle mechanism for electrons in the gaps between the wires. In the present OPV example, the entire system is a solid state device, and establishing electrical contact between the two wires must be done mechanically along their entire length. We demonstrated that the only practical means of accomplishing this is to wrap one wire around the other. Hence, the secondary electrode wire is wrapped around the coated primary wire (note: the wires are not twisted around one another) in a precisely controlled manner by means of a rotating stage upon which the spool of secondary wire is mounted. This process is similar to that used in commercial wire winding operations. An optical microscope picture of the wrapped pair is shown in Figure 4(a). The secondary electrode wire makes two complete wraps per inch of primary wire. Maintaining electrical contact is accomplished by keeping the wrapped pair under tension while pulling them through a coating cup containing a solvent-less, liquid pre-polymer of the protective outer cladding which is a photocurable epoxide. Immediately upon exiting the coating cup the liquid-clad wires enter a UV irradiation chamber which rapidly polymerizes and hardens the cladding. A digital microscope picture of a polymer-clad double wire is shown in Figure 4(b). Figure 4(c) is an electron micrograph image of the clad double wire. Figure 4(d) is an image of a spool containing 500 feet of the clad double wire. These spools are made in a continuous process similar to that used in the optical fiber industry; the process is capable of producing any length of wire desired.

### 1.2 OPV Wire Performance and Characterization

The photovoltaic performance of the OPV wire was determined in a manner that is very similar to that used for flat cells and modules. Lengths of wire ranging from one half to several feet cut from the large spool are placed in a calibrated solar simulator with an irradiance of 100 mW/cm$^2$ at AM1.5. Raw data from the solar simulator is corrected for the spectral mismatch of P3HT/PCBM via external quantum efficiency measurements resulting in ∼5% deviation to the true AM 1.5 values. Furthermore, the instrument is cross calibrated by re-measuring organic solar cells which were earlier certified by NREL and AIST.

The area of the wire is taken as its length multiplied by the diameter of the primary electrode wire, e.g., 100 $\mu$m, which is the projected area. No corrections are made for optical losses or gains from reflections from the curved air/cladding interface, the curvature of the primary wire, or for shadowing from the spiral-wrapped secondary electrode wire which is estimated to be 32% (Fig. 3b). This number



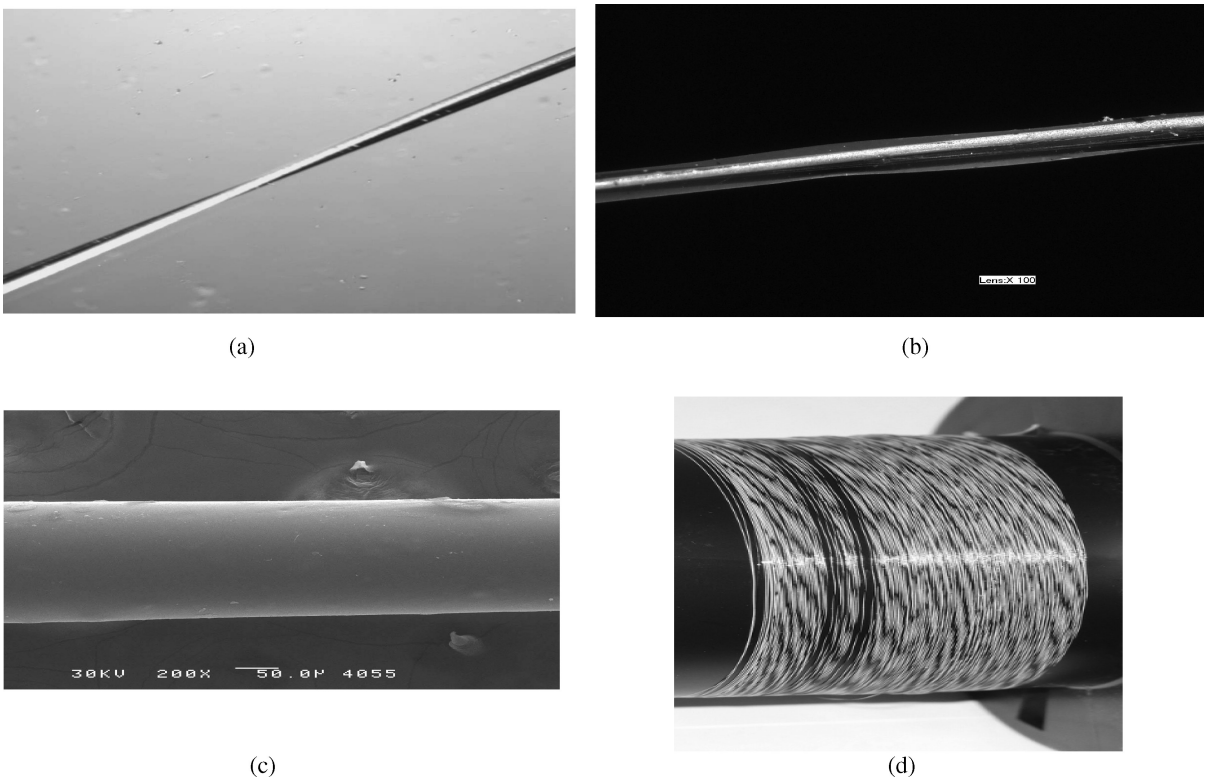


**Fig. 4.** (a) Optical microscope picture of the silver-coated, secondary electrode wire (white) wrapped around the coated, primary electrode wire before cladding; (b) digital microscope picture of a polymer clad double wire; (c) SEM of a polymer clad, double wire; (d) a spool containing 300 continuous feet of finished photovoltaic wire.

is obtained by calculating the projection of the secondary electrode wire on the primary electrode wire. Shadowing may be altered by simply changing the pitch of the latter. Modeling of this optically complex structure is discussed in the next section. Current-voltage curves (I-V curves) were determined after stripping the cladding from one of the ends of the wire, removing the photoactive layers from the primary electrode wire and making electrical connections to the solar simulator with alligator clips.

The process for generating photoactive, clad wires has been developed to the point where it is now capable of routinely producing several hundred feet of PV wire for any given experiment. Current-voltage curves of wire samples selected randomly from sections of these long wires exhibit an average efficiency of 2.99% (range 2.79–3.27%). When the geometry of the coaxial wires is adjusted so that the counter electrode wire does not shadow the primary electrode, the efficiency is 3.87%; a current voltage curve of this cell is shown in Figure 5. Many of these cell parameters are equivalent to those exhibited by flat cells. For example, the open circuit voltage (Voc) is >0.6mV, and the short circuit current density is 11.9mA/cm$^2$. The current density in high performance flat cells with the same materials in the active layer is usually in the range of 10–11mA/cm$^2$; the highest reported is 11.5 mA/cm$^2$ (20). The origin of this unexpectedly high value exhibited by the wire is related to the optics of the double wire system and will be discussed below. Both of these voltage and current should improve by the use of new polymers and fullerene derivatives that are currently under development in Konarka's laboratories. The parameter responsible for reducing the efficiency is the fill factor (FF = 53.8%) which in flat cells is typically around 0.6. Improvements to this parameter will be realized when the tensioning and cladding steps are optimized providing more effective electrical contact between the primary and secondary electrodes.

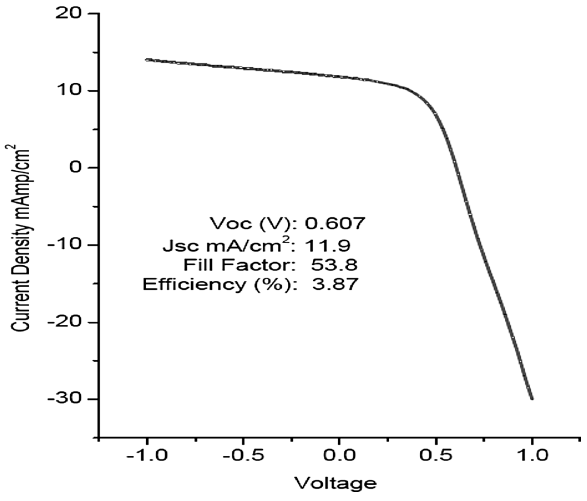


**Fig. 5.** I-V curve for a PV wire with the best performance observed thus far.

The optical properties of the cladding along with the geometry of this co-axial wire system were examined in order to gain insight into the origin of the unexpectedly high current density and to aid in devising a strategy for improving light management and performance. The first consideration centered on lensing and internal reflections from the cladding, as well as shadowing and diffuse reflections from the secondary electrode.

Ray tracing analysis was done in order to evaluate the amount of light incident on the active layer coated wire when it is shadowed to various levels by the spiral wrapped counter electrode wire. The geometry of the model used for this analysis comprises two circular cylinders, representing the electrode wires, embedded in an elliptical cylinder of transparent cladding (refractive index = 1.49); this is an accurate representation of the shape of polymer cladding at any position along the wires. Light striking the primary electrode is assumed to be completely absorbed while the silver-coated, counter electrode acts as a diffuse reflector; the silver coating has a measured diffuse reflectivity ranging from 42–54% across the visible spectrum. Since the counter electrode wire is spirally wound around the primary electrode wire (2 wraps/inch), shadowing of the latter ranges from complete shadowing to no shadowing. In this model, the width of the light source is held constant and set equal to the long axis of the ellipse (Fig. 6a, b).

Figure 6c shows the estimated percent of the power absorbed by the primary electrode as a function of the position of the counter electrode. When the counter electrode completely shadows the primary, e.g., 0° and 360°, the cladding focuses the incident light onto the primary wire which allows it to capture 30% of the incident radiation (green line) compared to 0% without the cladding (blue line). At 180°, where the primary electrode faces the incident light source, the cladding focuses the light and improves incident power absorption by 18% compared to the unclad fiber, e.g., 51% versus 33%, respectively. It should be noted that at angles between 0°, 180°, and 360°, the power captured by the primary wire is partially due to light reflected from the counter electrode. The measured reflectivity is 40%. This effect is particularly noticeable in the example of the unclad wires where a maximum occurs in the range of approximately 100°–140° and 220°–260°. For the clad wires, this effect is evidenced by the shoulders in the same range of angles. The results clearly indicate that shadowing by the counter electrode is partially compensated by the lensing effect of the cladding and, to a lesser but non-negligible extent, by diffuse reflection from the counter electrode.

Modeling strategy indicates that an improvement in light management with a concomitant enhancement in performance may be accomplished by increasing the size and refractive index of the cladding and by decreasing the diameter of the counter electrode. Increasing the size of the cladding from its current 200 $\mu$m to 300 $\mu$m combined with an increase in its refractive index from 1.49 (polyacrylate)

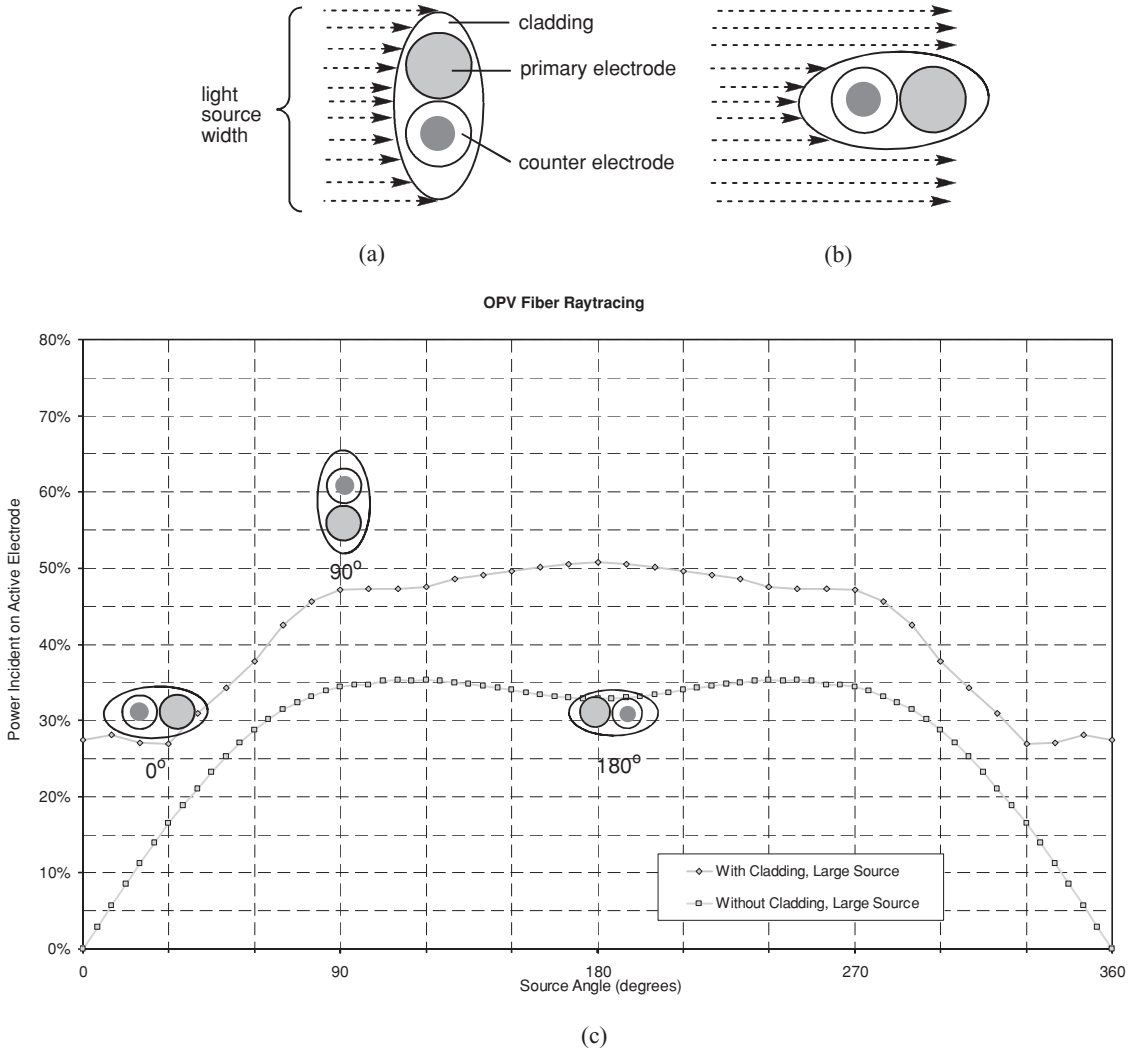


**Fig. 6.** (a) Light source equal to long axis of cladding ellipse; (b) Width of light source remains constant as the spiral-wrapped counter electrode wire rotates through 360°; (c) Demonstrates the power absorbed by the primary electrode wire as a function of the position of the spiral-wrapped counter electrode wire.

to 1.59 (polystyrene) will increase the amount of energy impinging the primary wire by 12% (Table 1). Decreasing the diameter of the counter electrode by half, from its current 100 $\mu$m to 50 $\mu$m, will result in another 7% increase in energy capture. Taken together these changes will improve energy capture by ∼20% to 1.59 (polystyrene) will increase the amount of energy impinging the primary wire by 12% (Table 1). Decreasing the diameter of the counter electrode by half, from its current 100 $\mu$m to 50 $\mu$m, will result in another 7% increase in energy capture. Taken together these changes will improve energy capture by ∼20%.

It is more difficult to illustrate the effect of the change in refractive index. The higher refractive index acts to increase the lensing effect from the cladding, further magnifying the absorptive wire and increasing its apparent size, and this results in an increase in the energy collected. The magnitude of this change is dependent on the cladding size used, and the data show that for larger cladding sizes a higher refractive index provides a greater return. For the current geometry, a change from acrylic cladding (n = 1.49) to polystyrene cladding (n = 1.59) results in less than a 2% relative improvement (shaded area in table). For a smaller secondary wire combined with a larger cladding size, the change in cladding materials results in a 6% improvement in collected energy (bold, italics in table).

Another approach to estimating the potential of this coaxial wire system is to determine the number of photons striking the active layer. This is accomplished by considering only two parameters: (i) the refractive index of the cladding and (ii) the distance of the point of incidence from the center of the fiber core. The photon count can be calculated by geometric optics; the transmission coefficients of the rays at the air-cladding-interface were determined via the Fresnel formulas. This allows for an estimation of the

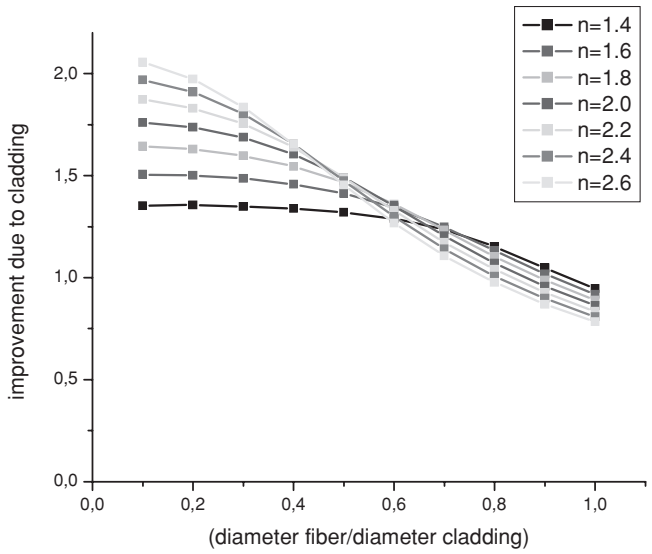


**Fig. 7.** Enhancement factor for the Jsc for different values of the refractive index of the OPV fiber and the ratio of the diameter of fiber and cladding.

**Table 1.** Average collected energy from OPV fiber as cladding material, cladding size, and reflective wire size are varied

| *Material* | *Secondary Wire Dia* | *Smaller Cladding* | *Nominal Cladding* | *Larger Cladding* |
|---|---|---|---|---|
| Acrylic | .0015″ | 0.3650 | 0.4169 | ***0.4261*** |
| SAN | | 0.3661 | 0.4345 | ***0.4450*** |
| Polystyrene | | 0.3664 | 0.4381 | ***0.4509*** |
| Acrylic | .002″ | 0.3393 | 0.4018 | 0.4075 |
| SAN | | 0.3331 | 0.4179 | 0.4267 |
| Polystyrene | | 0.3305 | 0.4212 | 0.4318 |
| Acrylic | .003″ | 0.3055 | 0.3762 | 0.3899 |
| SAN | (nominal) | 0.3016 | 0.3835 | 0.4095 |
| Polystyrene | | 0.3004 | 0.3847 | 0.4149 |
| Acrylic | .004″ | × | 0.3572 | 0.3676 |
| SAN | | × | 0.3618 | 0.3836 |
| Polystyrene | | × | 0.3626 | 0.3887 |
| Acrylic | .006″ | × | × | 0.3527 |
| SAN | | × | × | 0.3687 |
| Polystyrene | | × | × | 0.3729 |



efficiency by plotting the "light management" factor in the photovoltaic wire as a function of the refractive index and the ratio of the primary wire diameter to the cladding diameter (Fig. 7). This factor is defined as the number of photons incident on the active layer of the wire with cladding, divided by the number of photons for a wire without cladding. When the ratio of the diameters is taken 0.5, e.g., the wire core is 100 micron, the cladding is 200 micron, a cladding with a refractive index of 1.6 gives a light management factor of 1.42, which means that it can enhance the number of photons impinging the photoactive wire by more than 40% relative to a cladding with a refractive index of 1.4. As in the previous example, this approach suggests that a larger cladding with a higher the refractive index will capture energy that would otherwise be lost.

In summary, light capture and management by this coaxial system is highly effective in spite of shadowing losses by the counter electrode wire, and it is one of the key factors in generating high current density and performance.

### 1.3 PV Fabric–Initial Results

Recently, 100 PV wires were embroidered parallel to one another into a four inch square cotton cloth leaving 90% of the wires exposed on one side (Fig. 8a). All of the individual wires produce power attesting to the mechanical robustness of the coatings. We are now investigating ways to make multiple connections mechanically. Another cloth of similar size was made comprising 9 wires, each of which are 12 inches long passed three times through the four inch

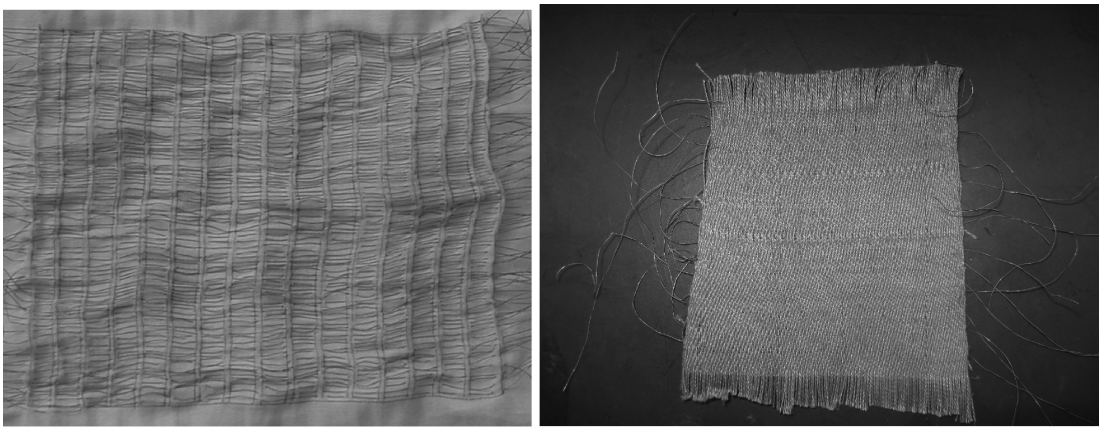

(a) (b)

**Fig. 8.** (a) PV wires embroidered into a cotton cloth exposing 90% of the wires; (b) wires woven with textile thread.

square fabric, all 9 wires were connected to one another in-series by hand. When exposed to 14,000 lumens, they produce enough power to turn on a small LED (1.3V). At full sunlight the voltage is 4.15V, and the current generated is 1.77 mA. Figure 8(b) is an image of a woven cloth made with brown inert textile thread and OPV wires. This fabric also powers an LED. These are the first examples of a photovoltaic fabrics.

## 2 Conclusions

Photovoltaic wires that produce electric current have been made by combining a primary electrode wire containing electron and hole injecting layers and the photoactive layer with a secondary electrode wire. The latter is wrapped around the primary wire making electrical contact, and the wrapped pair is coated with a transparent, photopolymer cladding which protects the PV coatings and helps ensure permanent contact between the two electrodes. The use of a highly conductive metal wire as the counter electrode in place of a transparent semi-conductor aids in current collection.

When exposed to simulated sunlight, the wires produce high voltage and current density. The efficiency of the best wire is 3.87%. Lensing and internal reflections combined with the refractive index and size of the cladding and the size of the counter electrode wire are important parameters for a efficient light management. The combined effects are able to over come shadowing by the counter electrode wire resulting in excellent performance.

Photovoltaic fabric has been made by weaving the wires with inert thread. The fabrics produce power when irradiated with sun light or incandescent light.



## Acknowledgements

The authors would like to acknowledge the ARMY Natick Soldier Center (Natick, MA) for financial support of this work and S. Fantone and H. Kent (Optikos Corporation, Wakefield, MA) for their helpful discussions and ray tracing analysis.

## References

1. Lewis, N.S. (2007) *Science*, 315, 798.
2. Lewis, N.S. and Crabtree, G. (Eds), Basic Research Needs for Solar Energy Utilization.(Report of the Basic Energy Sciences Workshop on Solar Energy Utilization, US Department of Energy, Washington DC, (2005); http://www.er.doe.gov/bes/reports/abstracts.html#SEU. (18–21 April, 2005).
3. (a) Yu, G., Gao, J., Hummelen, J.C., Wudl, F. and Heeger, A.J. (1995) *Science,* 270, 1789; (b) Yu, G. and Heeger, A. (1997) *Synthetic Metals,* 85, 1183
4. Schmidt-Mende, L., Fechtenkotter, A., Mullen, K., Moons, E., Friend, R.H. and MacKenzie, J.D. (2001) *Science*, 293, 1119.
5. Kim, Y., Cook, S., Tuladhar, S.M., Choulis, S.A., Nelson, J., Durrant, J.R., Bradley, D.D.C., Giles, M., McCulloch, I., Ha, C.-S. and Ree, M. (2006) *Nature Matls. Lett*., 5, 197.
6. Kim, J.Y., Lee, K., Coates, N.E. Moses, D. Nguyen, T.-Q., Dante, M. and Heeger, A.J. (2007) *Science,* 317, 222.
7. Peet, J., Kim, J.Y., Coates, N.E., Ma, W.L., Moses, D., Heeger, A.J. and Bazan, G.C. (2007) *Nature Materials,* 6, 497.
8. O'Regan, B. and Graetzel, M. (1991) *Nature,* 353, 737.
9. Huynh, W.U., Dittmer, J.J. and Alivisatos, A.P. (2002) *Science,* 295, 2425.
10. (a) Sarifciftci, N.S., Smilowitz, L., Heeger, A.J. and Wudl, F. (1992) *Science,* 258, 1474; (b) Sarifciftci, N.S. and Heeger, A.J. US Patents 5,454,880 and US 5,331,183.
11. Scharber, M.C., Mühlbacher, D., Koppe, M., Denk, P., Waldauf, C., Heeger, A.J. and Brabec, C.J. (2006) *Adv. Mater*., 18, 789.
12. Dennler, G., Scharber, M.C., Ameri, T., Denk, P., Forberich, K., Waldauf, C. and Brabec, C.J. (2008) *Adv. Mater.,* 20, 579.
13. Kayes, BM., Atwater, H. and Lewis, N.S. (2005) *J. Appl. Phys.,* 97, 114302.
14. Zhang, Y., Wang, L.W. and Mascarenhas, A. (2007) *Nano Lett.,* 7, 1264–1269.
15. Tian, B., Zheng, X., Kempa, T.J., Fang, Y., Yu, N., Yu, G., Huang, J. and Lieber, C.M. (2007) *Nature*, 449, 885.
16. (a) Ramier, J., Da Costa, N., Plummer, C.J.G., Leterrier, Y., Manson, J.-A.E., Eckert, R. and Gaudiana, R. (2008) *Thin Solid Films,* 516, 1913; (b) Ramier, J., Plummer, C.J.G., Leterrier, Y., Manson, J.-A.E., Eckert, R. and Gaudiana, R. (2008) *Renewable Energy,* 33, 314.
17. DSSC double wires comprising metal core electrode (5cm long x 75um diameter) and a secondary electrode wire reportedly exhibited <1% efficiency. Fan, X., Chu, Z., Wang, F., Zhang, C., Chen, L., Tang, Y., Zou, D. (2008) *Adv. Mater*., 20, 592.
18. (a). Describes concentrically deposited layers with a semi-transparent electrode with an efficiency <1%. O'Connor, K.P., Pipe, M. Shtein, *Appl. Phy. Lett.*, 92, 193306 920080; (b) Describes the use of a glass core with outer electrode with an efficiency ~3%. Liu, J., Namboothiry, M.A.G., Carroll, D.L. (2007) *Appl. Phy. Lett*., 90, 133515
19. Lee, M.R., Eckert, R.D., Forberich, K., Dennler, G., Brabec, C.J. and Gaudiana, R.A. (2009) *Science*, 324, 232.
20. Irwin, M.D., Buchholz, D.B., Hains, A.W., Chang, R.P.H. and Marks, T.J. (2008) *Proceedings Nat'l Acad. Sci.*, 105, 2783.